Atmos. Chem. Phys. Discuss., 11, 30563–30598, 2011
www.atmos-chem-phys-discuss.net/11/30563/2011/
doi:10.5194/acpd-11-30563-2011
© Author(s) 2011. CC Attribution 3.0 License.

Atmospheric Chemistry and Physics Discussions

This discussion paper is/has been under review for the journal Atmospheric Chemistry and Physics (ACP). Please refer to the corresponding final paper in ACP if available.

Improving $PM_{2.5}$ retrievals in the San Joaquin Valley using A-Train Multi-Satellite Observations

A. W. Strawa[1], R. B. Chatfield[1], M. Legg[2], B. Scarnato[3], and R. Esswein[2]

[1]NASA Ames Research Center, Moffett Field, California, USA
[2]Bay Area Environmental Research Institute, Sonoma, California, USA
[3]Oak Ridge Associated Universities, Oak Ridge, TN, USA

Received: 28 July 2011 – Accepted: 23 September 2011 – Published: 14 November 2011

Correspondence to: A. W. Strawa (anthony.w.strawa@nasa.gov)

Published by Copernicus Publications on behalf of the European Geosciences Union.

Abstract

This paper demonstrates the use of a combination of multi-platform satellite observations and statistical data analysis to dramatically improve the correlation between satellite observed aerosol optical depth (AOD) and ground-level retrieved $PM_{2.5}$. The target area is California's San Joaquin Valley which has a history of poor particulate air quality and where such correlations have not yielded good results. We have used MODIS AOD, OMI AOD, AAOD (absorption aerosol optical depth) and NO_2 concentration, and a seasonal parameter in a generalized additive model (GAM) to improve retrieved/observed $PM_{2.5}$ correlations (r^2) at six individual sites and for a data set combining all sites. For the combined data set using the GAM, r^2 improved to 0.69 compared with an r^2 of 0.27 for a simple linear regression of MODIS AOD to surface PM. Parameter sensitivities and the effect of multi-platform data on the sample size are discussed. Particularly noteworthy is the fact that the PM retrieved using the GAM captures many of the PM exceedences that were not seen in the simple linear regression model.

1 Introduction

Air quality in the United States has generally improved since the Air Pollution Control Act of 1955 was enacted. It is, however, still a concern in many regions of the country and in the world primarily because of its affect on human health (Samet et al., 2000; Pope et al., 2009; Krewski et al., 2009). Indirect calculations have pointed to an approximate loss of 1 year of life expectancy that can be attributed to long-term exposure to fine-particulate matter at a concentration of $10\,\mu g\,m^{-3}$ (Pope et al., 2009). The EPA National Ambient Air Quality Standard is a 24-h average (resp. annual average) $PM_{2.5}$ (mass concentration of airborne particles with an aerodynamic diameter of less than 2.5 µm) value below $35\,\mu g\,m^{-3}$ (resp. $15\,\mu g\,m^{-3}$). Although there are approximately 1600 EPA $PM_{2.5}$ approved monitoring sites throughout the United States since these

ACPD
11, 30563–30598, 2011

are ground based point measurements, there are many areas where there are huge gaps between measurements.

The idea of using satellite measurements to fill in the gaps between ground sensors has been an area of active research since 2003 when the first two studies on this topic were published (Wang and Christopher, 2003; Chu et al., 2003). Several satellite instruments measure the spectral extinction of light as it travels through the Earth's atmosphere. This unitless quantity called aerosol optical depth (AOD) is used to infer the amount of suspended aerosols in the total atmospheric column. While it is the surface measurement of particulate mass that is used for regulatory purposes, satellite observations of AOD have some advantages over surface measurements. They can provide better spatial coverage of pollutant in remote and non-monitored areas, track pollution transport, validate and guide model predictions, and suggest the placement of future surface sensors. Researchers have also been working to use satellite observations to improve air quality forecasts and to provide information to assist regulators and policy makers (Al-Saadi et al., 2005). The question we must answer to determine the utility of remote sensing data for particulate air quality monitoring is, "How well do the column measurements of AOD represent $PM_{2.5}$ concentrations at the ground?" While much progress has been made over the last decade, there is still much work to be done (Hidy et al., 2009; Hoff and Christopher, 2009).

To be useful for air quality purposes, satellite observations are (1) validated using ground-based AOD measurements from the globally distributed AErosol RObotic NETwork (AERONET), (2) translated to surface $PM_{2.5}$ measurements and (3) those "retrieved" mass concentration values must be validated against surface $PM_{2.5}$ measurements. Many studies use a single-variate, least-squares linear regression (a simple linear regression) to relate AOD with PM. Correlations in these studies show a considerable variation with correlation coefficients (r^2) between 0 and 0.85 depending on the season and location, or region, of comparison. Hoff and Christopher (2009) review and discuss over 30 papers that have explored the relationship between surface PM and satellite AOD measurements. Satellite AOD measurements from MODIS (MODerate

ACPD
11, 30563–30598, 2011

resolution Imaging Spectroradiometer), MISR (Multi-angle Imaging SpectroRadiometer), POLDER (POLarization and Directionality of Earth's Reflectance), and GOES (Geostationary Operational Environmental Satellite) have been used in these comparisons. For example, Gupta et al. (2006) investigated linear correlations between MODIS AOD and $PM_{2.5}$ at 25 urban areas globally and found correlations varied between 0.11 and 0.85. They found that the AOD-$PM_{2.5}$ relationships depended strongly on aerosol concentrations, ambient relative humidity, and height of the mixing layer. Kacenelenbogen et al. (2006) used simple linear regressions to compare POLDER AOD that is retrieved from spectral, directional, and polarized characteristics of the solar radiation and surface $PM_{2.5}$ measurements over France to obtain a correlation coefficient of 0.55 for the general area and 0.80 for particular sites. In some cases, notably in the western US, there is little or no correlation (Al-Saadi, et al., 2005; Engel-Cox, et al., 2004; Kahn et al., 2005; Gupta et al., 2006). Hoff and Christopher (2009) suggest that the poorer correlations in the West were due to a wider variation in aerosol types (more nitrate than sulfate and more biomass burning smoke than over the Eastern part of the United States.), higher surface reflectivity making passive satellite AOD retrieval difficult, and more elevated plumes in the AOD signatures. In general, satellite retrievals of AOD are most accurate over areas of dark vegetation (Levy et al., 2010). Not surprisingly, AOD-$PM_{2.5}$ correlations are poorest in areas where the AOD retrievals themselves are poor. Additionally, elevated aerosol plumes, typically associated with long-range transport, are integrated into the column AOD retrieval but are not reflected in the surface PM measurements.

Many schemes have been applied to improving satellite-surface correlations. Satellite AOD measurements have been combined with other parameters, such as the vertical structure of aerosol as calculated from a chemical transport model (van Donkelaar et al., 2010; Liu et al., 2009a), or estimates of boundary layer height and relative humidity from models (Liu et al., 2005, Kacenelenbogan et al., 2006). Liu et al. (2009b) used fractional component AOD from MISR (Multiangle Imaging Spectrometer) and aerosol vertical distributions from the GEOS-Chem transport model to constrain esti-

ACPD
11, 30563–30598, 2011

mates of surface $PM_{2.5}$. Liu et al. (2009b) used generalized linear regression models (GLM) and model-generated meteorological fields to compare the ability of MISR and MODIS AOD to predict surface $PM_{2.5}$ in the St. Louis region during 2003. The correlation coefficient between retrieved and measured PM using a GLM was $r^2 = 0.62$ and $r^2 = 0.51$ for MISR and MODIS, respectively.

Since many different parameters influence the PM-AOD relationship (for example, various measurements of AOD and Ångström exponent), another way to proceed is to adopt a statistical approach. Gupta et al. (2008) used multiple linear regression (MLR) and neural network techniques to include PBL height, location, temperature, and RH in an analysis in the southeastern US and achieved an improved r^2 of 0.7 using MLR and 0.83 using NN compared with r^2 of 0.41 for a simple linear regression model. Pelletier et al. (2007) applied GAM techniques to retrieve PM from the combination of AERONET AOD and NCEP meteorological data and compared with surface PM collected at two sites in northwestern Europe. Their model increase r^2 to 0.76 compared to an r^2 of 0.27 derived from a simple linear regression. Then Vidot et al. (2007) used the Pelletier et al. GAM method to relate surface PM with SeaWiFS (SeaWide Field-of-view Sensor), AOD, and National Center for Environmental Prediction (NCEP) meteorological parameters achieving an r^2 of 0.61 compared with 0.48 for the linear case.

$PM_{2.5}$ concentrations are needed in all weather conditions and at all locations and air quality models are used to "fill in the gaps" from satellite observations or surface stations. These models typically get their meteorological parameters from forecast, transport, or assimilation models and need to be validated. Using these same inputs in the $PM_{2.5}$ satellite retrievals would impugn the value of these retrievals in the validation process. Therefore, our objective in this paper is to improve estimates of $PM_{2.5}$ using only satellite observations and statistical techniques.

The study area, data sets, and methodology are discussed in the next section of this paper. Particular attention is paid to the generalized additive models (GAM) used in this research. Results of the GAM applied to six individual sites in the San Joaquin Valley (SJV) are presented and compared to the simple linear regression as a standard

ACPD
11, 30563–30598, 2011

metric. Then results from a case combining all 6 sites are described. One advantage of GAM over other statistical techniques is that general spline functions can be used to model the sensitivity of parameters on the $PM_{2.5}$ response. These sensitivities are discussed in the next section. The effect of adding satellite observations on sample size is discussed. Finally, time lines of $PM_{2.5}$ retrieved with a linear model and the GAM are compared with surface measurements.

2 Methodology

2.1 Study area

California's San Joaquin Valley (SJV) is located southeast of San Francisco in the center of the state between the Coastal Mountain Range to the west and the Sierra Nevada Range to the east (see Fig. 1). This topography leads to northwesterly winds during the spring, summer, and fall and a thick well-mixed boundary layer. During the winter, the winds die down and cold temperatures form an inversion layer keeping the boundary layer low and inhibiting surface mixing. The SJV encompasses nearly 64 000 km^2 and contains a population of over 3 million. Fresno, located in the center of the SJV, has a population of more than 500 000 and experiences frequent hospitalizations for asthma (Watson, 2000). From 1991 to 1996, $PM_{2.5}$ annual averages ranged from 18 to 24 $\mu g\,m^{-3}$ with the highest 24-h averages ranging from 56 to 93 $\mu g\,m^{-3}$. The 24-h averages exceeded the National Ambient Air Quality Standards (NAAQS) for $PM_{2.5}$, which are 15.0 $\mu g\,m^{-3}$ for the annual average and 35 $\mu g\,m^{-3}$ for the 24-h average. The highest $PM_{2.5}$ concentrations are typically found during the winter and fall. The winter and fall are also characterized by high concentrations of NH_4NO_3. Watson et al. (2000) provide an excellent overview of the Fresno air quality and air quality measurements made at the Fresno supersite.

Elevated concentrations of $PM_{2.5}$ can be associated with about 18 000 (ranging from 5600 to 32 000) premature deaths in California each year based on 2004–2006 air

ACPD
11, 30563–30598, 2011

quality data (Tran et al., 2009). Ground-based measurements are sparse in California and do not provide enough coverage for air quality monitoring. Further, there is little or no correlation between MODIS AOD and surface PM measurements in this region using single-variate, least-squares linear regressions (Engel-Cox et al., 2004). Previous attempts to improve this correlation by taking into account surface reflectance included in the MODIS Deep Blue retrieval for bright surfaces (Hsu et al., 2006) versus the standard MODIS dark target retrieval models have met with little success (Ballard et al., 2008; Justice et al., 2009). We have concentrated our study in the SJV.

2.2 Surface data

The California Air Resources Board (CARB) has established air quality monitoring stations throughout California. Air quality indicators such as chemical compounds and particulate matter concentrations, ozone levels, and meteorological conditions are monitored (Bucsela et al., 2008). The sties used for this study are listed in Table 1 and shown in Fig. 1.

While the Federal Reference Method (FRM) gravimetric filter-based samplers are the only samplers currently approved to provide data for determining the attainment status for an area, continuous mass monitors are used to collect data for understanding the diurnal and episodic behavior of fine particles, transport assessment, and for use by health scientists investigating exposure patterns.

In this study we use $PM_{2.5}$ obtained using both the FRM filter method for daily PM and the beta attenuation monitor (BAM) for the hourly PM. BAM measurements are a confirmed US Federal Equivalence Measurement relative to the 24-h filter-based reference standard (Zhu et al., 2007). The BAM determines the deposited mass by the attenuation of high-energy electrons through the sample filter. Accuracy is estimated to be ±8 % of indication for hourly readings and ±2 % for daily readings when compared to the FRM measurements (Ecotech, 2006).

Hourly $PM_{2.5}$, daily $PM_{2.5}$ averages, and daily PM_{10} averages were collected from July 2002 to July 2008 (http://www.arb.ca.gov/aqd/aqdcd/aqdcddld.htm). All available

ACPD
11, 30563–30598, 2011

$PM_{2.5}$, collected from 1 January 2007 to 6 July 2008 for each site, were obtained using the organization's online "Real-Time Query Tool": http://www.arb.ca.gov/aqmis2/paqdselect.php. All available relative humidity data, collected since 2002, were gathered using CARB's "Meteorological Data Query Tool": http://www.arb.ca.gov/aqmis2/metselect.php.

2.3 Satellite data

The satellite data used in this study come from the Ozone Monitoring Instrument (OMI) onboard NASA's EOS-Aura (Earth Observing System-Aura) satellite and the Moderate Resolution Imaging Spectroradiometer (MODIS) onboard NASA's EOS-Aqua (Levelt et al., 2006). Aqua and Aura were launched into a sun-synchronous orbit on 4 May 2002 and 15 July 2004, respectively. Aqua observes the SJV between 1300 and 1400 h, Pacific Standard Time. There is an approximate ~8 min time lapse between the AQUA and AURA overpasses. MODIS AOD was for this study because of its good spatial resolution, effective cloud mask algorithms, and its near-daily global coverage.

MODIS continuously acquires daily global measurements with 36 spectral bands (from 0.41 to 14 µm) at three different spatial resolutions (250 m, 500 m and 1 km). AOD is reported at $10 \times 10\,km^2$ resolution. MODIS' high spatial and temporal resolutions are well-suited for evaluating air quality on local, regional, and global scales (Levy et al., 2007a, b). The MODIS data products used in this study were the Level II Aerosol Product, Corrected Optical Depth Land, Surface Reflectance Land, Quality Assurance Land, Deep Blue Aerosol Optical Depth 550 Land (at 550 nm wavelength), Deep Blue Aerosol Optical Depth Land, Deep Blue Surface Reflectance Land, and Optical Depth Land and Ocean. Both the standard MODIS dark target and the Deep Blue Algorithm require a surface reflectance value to retrieve AOD values. The standard MODIS AOD retrieval algorithm uses the dark-target approach over land. "The Collection 5 land surface parameterization is based on the empirical relationships found between surface reflectance measured in the visible channels and at 2.13 µm. The relationships are a function of geometry and a mid-IR vegetation index measuring the greenness of the

ACPD
11, 30563–30598, 2011

vegetation (Levy et al., 2007)". This algorithm is accurate for determining AOD above highly vegetated surfaces, but performs poorly over highly reflective surfaces such as cities and deserts. The Deep Blue algorithm has proven to be successful at deriving AOD values over bright surfaces such as deserts (Hsu et al., 2006). Deep Blue uses a set of lookup tables based on a polarized radiative transfer model, allowing it to simulate the radiance for "a range of solar and viewing geometries at the top of the atmosphere" (Hsu et al., 2004). The MODIS dark target AOD product retrieves within an expected error envelope of $\pm(0.05 + 15\,\%)$ at 550 nm (Levy et al., 2010).

The OMI is an imaging spectrometer that measures solar light backscattered by the Earth's atmosphere and surface (Bucsela et al., 2006). The instrument consists of two spectrometers, one measuring the UV spectral range from 270 to 365 nm in two sub-ranges (UV1: 270–314 nm, resolution: 0.42 nm, sampling: 0.32 nm; UV2: 306–380 nm, resolution: 0.45 nm, sampling: 0.15 nm), the other measuring the UV-visible spectrum from 350 to 500 nm (resolution: 0.63 nm; sampling: 0.21 nm). OMI uses a CCD array with one dimension resolving the spectral features and the other dimension allowing a 114° field of view, providing a 2600-km viewing swath transverse to the orbit track. Its nadir spatial resolution ranges from 13×24 to $24 \times 48\,km^2$, depending on the instrument's operating mode. For this study we used OMI aerosol optical depth, aerosol absorption optical depth (AAOD), and NO_2, data product version 3. Good agreement is generally seen between the OMI and ground-based measurements, with tropospheric columns underestimated by 15–30 % (Celarier et al., 2008).

2.4 Data preparation

Satellites provide AOD usually only once a day and correlations are typically better with hourly rather than daily $PM_{2.5}$ surface measurements (Gupta et al., 2008; Ballard et al., 2008; Justice et al., 2009). The best correlation between MODIS AOD and surface $PM_{2.5}$ for sites in the SJV was found when averaging 5×5 10 km pixels centered at the ground station using a linear regression (Ballard et al., 2008; Justice et al., 2009). Comparing the average of a 5×5 pixel area AOD with hourly $PM_{2.5}$ measurements is

ACPD
11, 30563–30598, 2011

the standard practice for such studies (Abdou et al., 2005; Ichoku et al., 2002; Kahn et al., 2005; Remer et al., 2005). Two studies suggest that a 5 × 5 pixel average is a good approximation for AOD and validated it against AERONET data collected within one hour of the MODIS overpass time (Anderson et al., 2003; Ichoku et al., 2002). This finding is supported by the observation that the average speed of aerosol transport in mid-troposphere over ocean is 50 km h^{-1} based on TOMS images. We therefore used this value in the present study. OMI already has a large pixel size so the single pixel OMI data was used in this analysis. Including only MODIS AOD points with "Good" or "Very Good" quality flags marginally improved correlation (Justice et al., 2009), but this also restricted the number of data points in the comparison, sometimes severely. It was decided to ignore the data quality flags for this project. The surface $PM_{2.5}$ measurement was taken at the nearest hour to the satellite overpass.

We used the same data sets when comparing linear and GAM retrievals. For example, we have PM and MODIS data at Fresno from 2002 to present, but OMI data was only available from 2004–2008, so the comparison in the results section between correlations using the linear model with AOD only and the GAM model which included OMI data are made for the period 2004–2008.

2.5 Relating PM and AOD

PM can be related to AOD through the relationship (Koelemeijer et al., 2006)

$$\mathrm{AOD}(\lambda) = \mathrm{PM} H f(\mathrm{RH}) \frac{3 Q_{\mathrm{ext,dry}}(\lambda)}{4 \rho r_{\mathrm{eff}}}. \quad (1)$$

where H is the layer over which the AOD is measured, $f(\mathrm{RH})$ is the ratio of ambient and dry extinction coefficients, $Q_{\mathrm{ext,dry}}$ is the extinction efficiency (a function of particle size, composition, and wavelength) , ρ is the particle density, and r_{eff} is the particle effective radius (the ratio of the third and second moments of the size distribution). Equation (1) shows that the relationship between PM and AOD is dependent on the

ACPD
11, 30563–30598, 2011

vertical distribution of particles in the atmosphere, their size and composition, and the efficiency with which they interact with light.

The particles measured in determining PM reside in the planetary boundary layer (PBL) whose height is a function of the local meteorology. In winter in the SJV, the PBL is small resulting in high concentrations of PM near the surface. In the summer, the PBL is larger, resulting in decreased concentrations of PM near the surface. The presence of $f(\mathrm{RH})$ in Eq. (1) shows that the surface RH also affects AOD since the uptake of water vapor onto particles increases their size and extinction coefficient. In this study, these meteorological effects are represented with a 'seasonality' parameter, θ, that is modeled as a simple function of 'day of year'. Admittedly, θ will not take into account episodes where large amounts of particles reside above the PBL, affecting AOD but not PM. Incorporating these occurrences in the present algorithm would likely improve results, however, information on the vertical distribution of particles in the atmosphere are not routinely available in the SJV from ground-based lidars and data from the space-based Calipso lidar is too infrequent for this study. Finally, particle and gas phase constituents are interrelated through the processes of nucleation, condensation, and evaporation. Therefore, a relationship between the satellite gas phase product and the PM response can reasonably be expected. In this study, column concentrations of NO_2 from the OMI satellite were found to be significant in the retrieval of PM.

2.6 Statistical methods

In a simple linear regression model, the relationship between a response y and parameters $x_1, \ldots, x_p$ is given by

$$y = B_0 + \sum_{j=1}^{p} B_j x_j + \varepsilon \quad (2)$$

ACPD
11, 30563–30598, 2011

where the B_j are constants and ε is the residual error. In the simplest case, when PM is compared with AOD only, Eq. (2) becomes:

$$PM_{2.5} = B_0 + B_1 AOD + \varepsilon. \quad (3)$$

In an additive model, we replace the linear relationship between the parameters and response with a functional relationship so that an additive model takes the form:

$$y = B_0 + \sum_{j=1} f_j(x_j) + \varepsilon \quad (4)$$

where the f_j are simple, smooth arbitrary functions replacing the coefficients B_j. Replacing the B_j with f_j is necessary because some parameters show a nonlinear dependency with $PM_{2.5}$. Some parameters may have a large effect on the response in only a particular part of their range. For example, a variable may be dominated by random error at very low values or have other undesirable effects at very high values, such as MODIS Deep Blue AOD as shown in Fig. 4a. For these reasons it is appropriate to make the simple extension of linear to non-linear regressions. Generalized additive models (GAMS) are such an extension, retaining additive terms (Wood, 2006, 2007).

In this case we employ several retrievals of AOD as parameters (e.g., MODIS standard algorithm, MODIS Deep Blue, OMI), because each has its possible virtues and range of greatest applicability. For example the OMI AAOD tends to be more sensitive to aerosols at high altitude.

Generalized additive models (GAMs) and neural network algorithms have been used previously but not with satellite-only data sets (Gupta, et al., 2006; Pelletier, et al., 2007; Vidot et al., 2007; Lary et al., 2009). Additive models provide flexibility but also allow functional forms to be plotted, allowing us to evaluate the physical rationale of the relationship expressed in the function. In this implementation we will use splines to describe the relationship between parameters and response in a functional form that can be related to a physical basis. The resulting predictive model is used to predict surface PM from satellite observations.

ACPD
11, 30563–30598, 2011

3 Results and discussion

3.1 Linear regressions between parameters

When a particular response, in this case PM, is a function of multiple parameters, it is instructive to explore the relationship between different parameters. This information can guide the selection of parameters to include in a multiple regression and help explain the results of the analysis. Correlations for the linear regressions between the parameters of interest in this study are shown in Table 2. These correlations are based on the data from all sites that form the complete set described in more detail in Sect. 3.2. Some features of the data in Table 2 stand out. First, there are excellent correlations between AOD retrieved by the same method or instrument at different wavelengths. For example, the correlation between MODIS AOD at 0.47 and 0.55 nm using the standard retrieval (AOD_47 and AOD_55) is 0.97. The correlation for the Deep Blue retrieval (DB_AOD_47 and D_AOD_55) was also 0.97. The high correlation between AOD at different wavelengths may be due to the constraints that the MODIS retrieval puts on the wavelength dependence. This practice is typical of other satellite retrievals This indicates that no new information will be obtained from including both wavelengths from the same retrieval. It is also interesting that the AOD retrieved using different methods does not correlate very well: the correlation between AOD_47 and DB_AOD_47 was 0.35; the correlation between AOD_47 and OMI AOD was 0.15; and the correlation between BD_AOD_47 and OMI AOD was 0.7. The correlation between OMI AOD and AAOD was 0.6. These low correlations are surprising. They suggest that the different retrieval algorithms play an important role in determining AOD. They also suggest that different retrievals or observations are providing different information about the aerosol optical depth. This may be because the measurements are made at different wavelengths (OMI observations are made at shorter wavelengths than MODIS) or different assumption for aerosol models or surface reflectance are used in the retrieval algorithm. The other surprising fact from the data in Table 2 is the generally low level of correlation between the other parameters. Low correlations between PM and satellite

ACPD
11, 30563–30598, 2011

observations in this region has been observed and commented on before.

3.2 Correlations for individual sites

As an example of how the GAM model can work for an individual site, we look at the Fresno site for four years, 2004–2008. Figure 2a shows a scatter plot of $PM_{2.5}$ modeled using a simple linear regression of MODIS Deep Blue AOD (DB_AOD_47) versus $PM_{2.5}$. The correlation coefficient, R^2, is 0.21. Note the lack of agreement especially for large values of $PM_{2.5}$. These are the most important points to match since they are associated with the exceedances of EPA criterion pollutant standards, which is 35 $\mu g\,m^{-3}$ for a 24-h average $PM_{2.5}$. Figure 2b shows a scatter plot of $PM_{2.5}$ modeled using a GAM for the same data. Parameters used in the model are MODIS Deep Blue AOD at 0.4 µm wavelength, OMI NO_2, and θ (day of year, a proxy for seasonal variation). The correlation coefficient has improved to $R^2 = 0.72$ for $PM_{2.5}$ measurements.

We see from Fig. 2a and b that a positive intercept is obtained using both the simple linear and GAM retrievals. It has been suggested that this intercept represents the minimum level of particle concentration for which the satellite-derived AOD is sensitive (Gupta et al., 2008). It is probably more suitable to claim the lowest reported value as the instrument sensitivity. In both cases this is about 12 $\mu g\,m^{-3}$.

Table 3 summarizes the results of the GAM model for six San Joaquin Valley sites: Bakersfield, Fresno, Modesto, Stockton, Turlock, and Tracy. In all cases the response was hourly $PM_{2.5}$ measured at the surface site. Very little Deep Blue AOD was available for Modesto, therefore, data from the standard algorithm was used. Results of the simple linear regression are shown in red for comparison. The number of points used in the correlation is listed and discussed later. The low number of points for Tracy is due to PM data only being available for part of one year, 2007. The correlation to daily PM is better for Bakersfield and Fresno than for the hourly PM.

The data show that there is general improvement in the correlations for the various sites over the simple linear regression. We explored many combinations of parameters

ACPD
11, 30563–30598, 2011

looking for the best fit of retrieved to measured PM. Better correlations were obtained using surface measurements of NO_x, but the objective in this study was to use only satellite observations since these are most transferable to non-monitored areas. The parameter set chosen for Table 3 was the set that gave the best performance for the entire SJV, however, some sites did have slightly better agreement than those listed in Table 3 with a different set of paramters.

3.3 Multiple-site retrieval

Our goal in this work is to obtain the best retrieved-PM for the entire SJV using only satellite observations. We combined all of our San Joaquin Valley sites into one data set. A parameter to differentiate between sites was included to account for topological and population differences but it had a negligible contribution to the retrieval and it was not included in the parameter sets considered here. Table 4 summarizes the results of several GAM models for the six San Joaquin sites. The best correlation ($r^2 = 0.74$) between observed and retrieved surface PM occurred when the GAM1 model was used. This model included all six parameters: MODIS standard AOD, MODIS Deep Blue AOD, OMI AOD, OMI AAOD, OMI NO_2, and θ. However, as discussed in Sect. 3.5, adding more parameters significantly reduced the sample size. In this case the sample size was reduced from 2122 to 630. To obtain the other retrieval models that make up Table 4, different parameters (indicated by an "X") were eliminated and retrievals obtained. The results of the correlation and effects on sample size are shown in Table 4. Then a scheme for combining several GAM models was devised which kept the sample size constant and had minimal effect on the correlation coefficient. We discovered that we could retain all 2122 sample points in this way and only reduce the correlation to 0.69. The combination was performed using the following steps:

1. The GAM1 model (see Table 4) was run with the full set of six parameters. The retrievals were weighted as described in Sect. 3.4.

2. Parameters were eliminated and the effect on correlation coefficient and sample

ACPD
11, 30563–30598, 2011

size was recorded. It was found using OMI AAOD as a parameter resulted in the largest decrease in sample size. Eliminating either the standard or Deep Blue MODIS AOD did not have a large effect on the correlations and reduced the number of sample points only slightly.

3. This procedure resulted in six models using six different sets of parameters. The 6 models and their results are shown in Table 4 along with a simple linear model for comparison and each parameter's p-value sensitivity.

4. The next step was to combine all six retrieval models ensuring that no data point was used more than once. The sample points were combined by taking the points from the model with the highest r^2 (GAM1) and adding the points from the model with the next highest r^2 (GAM3) that were not contained in the previous model. Points from the remaining models were added in this same fashion.

5. The combined data set r^2 was determined and shown in Table 4.

The values listed in the row across from the parameters are their p-value. P-value is a measure of how significant a parameter is in the retrieval. The smaller the p-value the more highly significant is the effect of the parameter in the model. (In statistical terms, the *p*-value is a measure of how much evidence we have against the null hypothesis; that is the assumption that the parameter has no effect on the retrieval.)

3.4 Weighting for PM exceedances

It is possible to weight the response when using regressions. In this case it was desirable to put more weight on higher PM values – those associated with EPA exceedances that are of more interest to the regulatory and epidemiology community. This was accomplished in this study using an iterative process. First the GAM models in Table 4 were run without weighting. Then the resultant retrieved PM values were used to establish a weighting and the GAM model was run again. Figure 3 shows the data correlations for the combined data set with a variety of models. Figure 3a is a simple

ACPD
11, 30563–30598, 2011

linear model correlating standard MODIS AOD with PM for reference. Figure 3b is the combined GAM model without weighting for PM, and Fig. 3c is a simple correlation for the weighted model results. It is seen that the r^2 has not changed between Figs. 3b and c. When using a weighting function, it is appropriate to look at the correlation as a function of the weighted variables. A standard correlation between two variables, x and y, is

$$\mathrm{COR} = \frac{\frac{1}{n}\sum\left[(x-\mu_x)(y-\mu_y)\right]}{\sigma_x \sigma_y} \tag{5}$$

where μ is the mean value and σ is the standard deviation of the parameter x or y. The weighting function, w_n, used was based on the retrieve values

$$w_n = \left(\frac{|\mathrm{retrieved_values}_n|}{\sum \mathrm{retrieved_values}}\right)^{0.5} \tag{6}$$

to insure that the weighting function was normalized, $\sum w_n^2 = 1$. Then the weighted correlation becomes

$$\mathrm{COR} = \frac{\frac{1}{n}\sum w_n^2\left[(x-\mu_x)(y-\mu_y)\right]}{\sigma_x \sigma_y} \tag{7}$$

Figure 3d shows the scatter plot for the weighted observed and retrieved PM. It is clear that weighting is doing a better job at matching the higher values of PM.

3.5 Parameter sensitivities

OMI NO_2 was a significant contributor to predicting PM and had a linear sensitivity with PM. This is probably because OMI NO_2 is a measure of how much the SJV is affected by NO_x-generating polluters, in this case, vehicle traffic. Nitrogen dioxide is formed in the environment from primary emissions of oxides of nitrogen. Although there are

ACPD
11, 30563–30598, 2011

natural sources of NO_x (e.g., forest fires), the combustion of fossil fuels has been, and remains, the major contributor in urban areas. Traffic pollution and power plants are two of the biggest sources of NO_2 pollution in the United States. Sulfate aerosol make up only about 5 % of the total aerosol in the Fresno area while nitrate makes up about 25 % and BC and OC make up about 18 % and 21 %, respectively (McMurry et al., 2004). We note that OMI NO_2 does not typically correlate well with surface measurements. We believe this is because the surface measurement is a point measurement, while the satellite data represents a more distributed value. Including surface reflectance in the model had very little effect on the agreement between retrieved and measured PM suggesting that the Deep Blue surface reflectance model is sufficient for the AOD retrieval in the SJV. Ångström exponent was not a significant parameter in any of the models. This was expected due to the high correlation between AOD at different wavelengths. As previously mentioned, one of the advantages of using GAMs in this application is that they produce plots of the relationships between the response (PM) and the parameters (e.g., AOD, NO_2) that can suggest a physical relationship. To illustrate, Fig. 4a shows the sensitivity of MODIS Deep Blue AOD with respect to PM. This sensistivity is the coefficient, f_j in Eq. (4), that corresponds to the parameter MODIS Deep Blue AOD. This sensitivity is nearly linear as one would hope, however there are some departures from linearity that are captured by the spline function.

The significance of the seasonal variation in the GAM models is large, as seen in the very low p-values in Table 4. This is expected because meteorological conditions strongly affect PM concentrations. These include: vertical mixing of air pollutants, temperature, moisture, long and short range transport, and the available sunlight which effect secondary organic aerosol. Liu et al. (2009b) discriminated between spring and non-spring seasons in their work using GAMs and model-generated meteorological fields. Figure 4b shows the seasonal sensitivity as function of day-of-year. In the SJV it is observed that very high levels of pollution occur on strong inversion days (Watson et al., 2000). Others have considered the factors affecting the air quality in the region (e.g., Chow et al., 2006), and found that motor vehicles and residential wood burn-

ACPD
11, 30563–30598, 2011

ing are the principal sources of aerosol particles. Emissions from motor vehicles are essentially constant during the year while wood burning emissions constitute a major aerosol mass fraction in the fall and winter seasons beginning mid-November. Presumably, residential wood smoke particulates would be minimal at 1400 the time of the satellite overpass. Justice et al. (2009) found that while surface measurements of $PM_{2.5}$ in SJV were greatest in the winter, AOD values were lowest in the winter. Investigating the relationship between sunphotometer-derived AOD to PM at Ispra, Italy, Barnaba et al. (2010) found a similar effect with maximum AOD occurring in spring/summer and maximum PM values occurring in winter. They were able to use coincident lidar measurements to demonstrate that the variation in aerosol vertical distribution was important in this discrepancy. Since there are no lidar sites in the SJV, we were unable to explore this phenomenon presenting the present study, however the statistical model was able to capture the proper seasonal behavior and successfully model it.

Given that PM is a dry measurement and AOD is not, the seasonal variation in RH may be reflected in the seasonal functional dependence. The choice of the day-of-year parameter was due to expedience. The influence of seasonal factors on surface PM, such as relative humidity, height of the planetary boundary layer, composition of the aerosol due to seasonal emissions, is well documented. We could obtain no reliable observations of these parameters from remote sources in keeping with our premise to use only remote observations to retrieve surface PM values. There was an attempt to use RH from assimilation models, but these proved to be inaccurate unless some modeled meteorology was included in the assimilation. Barnaba et al. (2010) found that the correlation did not improve when RH was considered. Similarly, for the few cases in which surface measurements of RH did exist, we found that they did not have a significant effect on the correlations between retrieved and measured PM. Additionally, the usefulness of our retrievals for validating model predictions of PM would be compromised if the same meteorological model was used in estimating RH. Thus the day-of-year parameter seemed the best choice for this study. The limitation with using day-of-year is that the meteorological factors that effect PM do not commence at the

ACPD
11, 30563–30598, 2011

same time every year. We are exploring ways to add this influence in our algorithm development.

3.6 Effect of adding parameters on sample size

The number of sample points decreases dramatically when PM is merged with satellite data. Hidy et al. (2009) note that for MODIS data in Fresno from 2002 to 2008, cloud-free days were available 43, 61, 94, and 81 % of the time in winter, spring, summer, and fall, respectively. Table 5 shows how the number of sample points decreases as more parameters are added. The data set is limited to days that have OMI data, from 1 Oct. 2004 to 6 Jul 2008. This gives a total of 8244 possible samples for six sites. Of these possible samples, MODIS data existed for 4455 points. But our criterion for averaging over the 5 × 5 pixels was that >50 % of the 25 pixels had to have valid data. This restriction is more severe than is typically used for these types of studies and (slightly) reduced the number of points to 4340. The reduction in points resulting from the merge with satellite data is largely due to cloudy pixels. Since OMI has a larger footprint than MODIS, the number of "cloudy" pixels is larger.

3.7 Retrieved and observed PM trends

To further illustrate the utility of the multi-satellite GAM retrieval, observed PM for days in our sample set are plotted with retrieved PM from a simple linear regression with standard MODIS AOD (Fig. 5a) and with the GAM-retrieved PM (Fig. 5b). The figures clearly illustrate that the GAM retrieval does a superior job in matching the observed PM and capturing exceedances. The lines in the plots are smoothed data to show trends.

Of the 1272 data points in the set, surface measurements recorded 149 exceedances. The linear fit recorded six and the GAM fit recorded 167. The GAM fit correctly identified 68 % of the exceedances, missed 31 %, and gave false positives for 43 %. While this is a big improvement, it underscores the fact that there is a long way

ACPD
11, 30563–30598, 2011

to go before surface measurements will be replaced by satellite retrievals for regulatory purposes. Thus we contend that the real near-term utility of satellite-derived PM will be in filling in the gaps of surface measurements to improved validation of air quality models and for epidemiology studies.

4 Conclusions

This paper demonstrates the use of GAM models with multi-platform satellite observations to dramatically improve the correlation between observed and retrieved PM in California's San Joaquin Valley. The parameters used are MODIS AOD, OMI AOD, AAOD and NO_2 concentration, and a seasonal parameter. Correlations (r^2) for the retrieved/observed $PM_{2.5}$ for a data set combining six surface sites improve to 0.69 compared with r^2 of 0.27 for the linear regression of MODIS AOD to surface PM. Particularly noteworthy is the fact that the PM retrieved using the GAM captures many of the PM exceedences that were not seen in the simple linear regression.

Further improvements are needed. The GAM models and input data can be refined by using other combinations of parameters and including more measurement sites, especially rural sites. Certainly, the inclusion of other available data, especially information on the vertical distribution of particles, when available, may further improve these results. The question of the generality of this technique needs to be addressed in the future. We intend to apply this technique to other areas globally that have similar topography to the SJV and that have demonstrated poor correlations between AOD and PM. We expect that the combinations of parameters used in the SJV will be useful in these areas. However, there may be some regions in which the combination of parameters needs to be adjusted. For example, NO_2 concentration was a significant factor in retrieving PM in the SJV, but this may have been due to the prevalence of transportation related emissions in the region. In other regions more heavily dominated by electrical power plant emissions, SO_2 may prove to be more significant than NO_2 in the retrievals. However, we feel that the techniques demonstrated in this study can

ACPD
11, 30563–30598, 2011

be used to greatly enhance the utility of satellite-retrieved PM for air quality purposes. In addition, the GAM model produces relationships between the parameters and the response that may lead to improved satellite retrieval of AOD, surface reflectance, etc.

Improved retrieved-$PM_{2.5}$ from satellite data will have profound benefits. They will be valuable in validating emission inventories used in global climate models and for validation of air quality models. They will be especially useful in sparsely populated regions where no data is available and areas where residents are exposed to significant $PM_{2.5}$ concentrations but where measurements are not available. Such data can be used to track pollution transport, suggest the placement of future surface monitoring stations, and in epidemiological studies that seek to identify the sources of the most toxic air pollutants and the susceptible populations. These techniques will prove useful in improving satellite observations of particulate as well as gas phase air quality, not only in the western United States, but globally.

Acknowledgements. MODIS data were obtained from the Goddard Earth Sciences (GES) Data and Information Services Center (DISC) and OMI data were obtained from the OMI International Science Team for the OMI satellite data.

We acknowledge the personnel of CARB for the effort required to collect the surface data used in this study. Much of the surface measurements used in this study were compiled by two teams of students working at Ames under the NASA DEVELOP program under the leadership of J. Skiles and C. Schmidt during the summer of 2008–2009. A. Strawa was the mentor for these groups.

We wish to acknowledge The MODIS and OMI teams for the use of their data products. Lorraine Remer and Richard Kleidman gave us valuable insight on the use of MODIS aerosol data products and on the techniques used in this study. Omar Torres gave us valuable insight on the use of the OMI aerosol data products.

References

Abdou, W. A., Diner, D. J., Martonchik, J. V., Bruegge, C. J., Kahn, R. A., Gaitley, B. J., Crean, K. A., Remer, L. A., and Holben, B. N.: Comparison of coincident Multiangle Imaging Spec-

ACPD

11, 30563–30598, 2011

troradiometer and Moderate Resolution Imaging Spectroradiometer aerosol optical depths over land and ocean scenes containing Aerosol Robotic Network sites, J. Geophys. Res., 110, 11967–11976, 2005.

Al-Saadi, J., Szykman, J., Pierce, R. B., Kittaka, C., Neil, D., Chu, D.A., Remer, L., Gumley, L., Prins, E., Weinstock, L., MacDonald, C., Wayland, R., Dimmick, F., and Fishman, J.: Improving national air quality forecasts with satellite aerosol observations, Bull. Amer. Met. Soc., 1249–1261, 2005.

American Ecotech Technical Report: Beta-attenuation mass monitor, 2006.

Anderson, T. L., Robert, J., Charlson, R. J., David, M., Winker, D. M., John, A., Ogren, J. A., and Holm'en, K.: Mesoscale Variations of Tropospheric Aerosols, J. Atmos. Sci., 60, 119–136, 2003.

Ballard, M., Newcomer, M., Rudy, J., Lake, S., Sambasivam, S., Strawa, A. W., Schmidt, C., and Skiles, J. W.: Understanding the correlation of San Joaquin air quality monitoring with aerosol optical thickness satellite measurements. ASPRS Annual Conference, Baltimore MD, 2008.

Barnaba, F., Putaud, J. P., Gruening, C., dell'Acqua, A., and Dos Santos, S.: Annual cycle in co-located in situ, total-column, and height-resolved aerosol observations in the Po Valley (Italy): Implications for ground-level particulate matter mass concentration estimation from remote sensing, J. Geophys. Res., 115, D19209, doi:10.1029/2009JD013002, 2010.

Bucsela, E. J., Celarier E. A., Weing, M. O., Gleason, J. F., Veefkind, J. P., Boersma, J. P., and Brinksma, E. J.: Algorithm for NO_2 vertical column retrieval from the Ozone Monitoring Instrument, IEEE T. Geosci. Remote, 44, 1245–1258, 2006.

California Air Resources Board, Emission Data by Region (Statewide), 2008.

Celarier, E. A., Brinksma, E. J., Gleason, J. F., Veefkind, J. P., Cede, A., Herman, J. R., Ionov, D., Goutail, F., Pommereau, J.-P., Lambert, J.-C., van Roozendael, M., Pinardi, G., Wittrock, F., Schönhardt, A., Richter, A., Ibrahim, O. W., Wagner, T., Bojkov, B., Mount, G., Spinei, E., Chen, C. M., Pongetti, T. J., Sander, S. P., Bucsela, E. J., Wenig, M. O., Swart, D. P. J., Volten, H., Kroon, M., and Levelt, P. F.: Validation of Ozone Monitoring Instrument nitrogen dioxide columns, J. Geophys. Res., 113, D15S15, doi:10.1029/2007JD008908, 2008.

Chow, J. C., Watson, J. G., Lowenthal, D. H., Chen, L.-W., Tropp, R. J., Park, K., and Magliano, K. A.: $PM_{2.5}$ and PM_{10} mass measurements in California's San Joaquin Valley, Aerosol Sci. Technol., 40, 796–810, 2006.

Chu, D. A., Kaufman, Y. J., Zibordi, G., Chern, J. D., Mao, J., Li, C. C., and Holben, B.N.:

ACPD
11, 30563–30598, 2011

Global monitoring of Air pollution over land fom the Earth Observing System-Terra Moderate Resolution Imaging Spectrometer (MODIS), J. Geophys. Res. Atmos., 108, 4661, doi:10.1029/2002jd003179, 2003.

Engel-Cox, J. A., Holloman, C. H., Coutant, B. W., and Hoff, R. M.: Qualitative and quantitative evaluation of MODIS satellite sensor data for regional and urban scale air quality, Atmos. Environ., 38, 2495–2509, 2004.

Goody, R. M. and Yung, Y. L.: Atmospheric Radiation, Theoretical Basis, 2nd edn., Oxford University Press, New York, USA, 1989.

Gupta, P. and Christopher, S. A.: Seven year particulate matter air quality assessment from surface and satellite measurements, Atmos. Chem. Phys., 8, 3311–3324, doi:10.5194/acp-8-3311-2008, 2008.

Gupta, P., Christopher, S. A., Wang, J., Gerhrig, R., Lee, Y., and Kumar, N.: Satellite remote sensing of particulate matter and air quality assessment over global cities, Atmos. Environ., 40, 5880–5892, 2006.

Hidy, G. M., Brook, J. R., Chow, J. C., Green, M., Husar R. B., Lee, C., Scheffe, R. D., Swanson, and Watson, J. G.: Remote sensing of particulate pollution from space: Have we reached the promised land?, J. Air & Waste Manage. Assoc., 59, 1130–1139, 2009.

Hoff, R. M., Christopher, S. A.: Remote sensing of particulate pollution from spcae: Have we reached the promised land?, J. Air Waste Manage. Assoc., 59, 645–675, 2009.

Hsu, N. C., Tsay, S.-C., King, M. D., and Herman, J. R.: Deep blue retrievals of Asian Aerosol properties during ACE-Asia, IEEE T. Geosci. Elect., 44, 3180–3195, 2006.

Hsu, N. C., Tsay, S.-C., and King, M. D.: Aerosol properties over birght-reflecting source regions, IEEE T. Geosci. Elect., 42, 557–569, 2004.

Ichoku, C., Chu, D. A., Mattoo, S., Kaufman, Y. J., Remer, L. A., Tanré, D., Slustsker, I., and Holben, B. N.: A spatio-temporal approach for global validation and analysis of MODIS aerosol products, Geophys. Res. Lett., 29, 1–4, doi:10.1029/2001GL013206, 2002.

Justice, E., Huston, L., Krauth, D., Mack, J., Oza, S., Strawa, A. W., Skiles, J. W., Legg, M., and Schmidt, C.: Investigating correlations between satellite-derived aerosol optical depth and ground $PM_{2.5}$ measurements in California's San Joaquin Valley with MODIS Deep Blue, ASPRS Annual Conference, Baltimore MD, 2009.

Kacenelenbogen, M., Léon, J.-F., Chiapello, I., and Tanré, D.: Characterization of aerosol pollution events in France using ground-based and POLDER-2 satellite data, Atmos. Chem. Phys., 6, 4843–4849, doi:10.5194/acp-6-4843-2006, 2006.

ACPD
11, 30563–30598, 2011

Kahn, R. A., Gaitley, B. J., Martonchik, J. V., Diner, D. J., and Crean, K. A.: Multiangle Imaging Spectroradiometer (MISR) global aerosol optical depth validation based on 2 years of coincident aerosol Robotic Network (AERONET) observations, J. Geophys Res., 110, D10S04, doi:10.1029/2004JD004706, 2005.

Krewski, D., Jerrett, M., Burnett, R. T., Ma, R., Hughes, E., Shi, Y., Turner, M. C., Pope, C. A., Thurston, G., Calle, E. E., and Thun, M. J.: Extended follow-up and spatial analysis of the American Cancer Society study linking particulate air pollution and mortality, Health Effects Inst. Research Rpt. #140, 2009.

Lary, D. J., Remer, L. A., MacNeill, D., Roscoe, B., and Paradise, S.: Machine learning and bias correction for MODIS aerosol optical depth, IEEE Geosci. Remote S., 6, 1–5, 2009.

Levelt, P. F., Hilsenrath, E., Leppelmeier, G. W., van den Oord, G. B. J., Bhartia, P. K., Tamminen, J., de Hann, J. F., and Veefkind, J. P.: Science objectives of the Ozone Monitoring Instrument, IEEE T. Geosci. Remote, 44, 1199–1208, 2006.

Levy, R. C., Remer, L., Mattoo, S., Vermote, E., and Kaufman, Y. J.: Second-generation algorithm for retrieving aerosol properties over land from MODIS spectral reflectance, J. Geophys. Res., 112, D13211, doi:10.1029/2006JD007811, 2007a.

Levy, R. C., Remer, L., and Dubovik, O.: Global aerosol optical properties and application to MODIS aerosol retrieval over land, J. Geophys. Res., 112, D13210, doi:10.1029/2006JD007815, 2007b.

Levy, R. C., Remer, L. A., Kleidman, R. G., Mattoo, S., Ichoku, C., Kahn, R., and Eck, T. F.: Global evaluation of the Collection 5 MODIS dark-target aerosol products over land, Atmos. Chem. Phys., 10, 10399–10420, doi:10.5194/acp-10-10399-2010, 2010.

Liu, Y., Sarnat, J. A., Kilaru, V., Jacob, D. J., and Koutrakis, P.: Estimating ground-level $PM_{2.5}$ in the Eastern United Sates using satellite remote sensing, Environ. Sci. Technol., 39, 3269–3278, 2005.

Liu, Y., Franklin, M., Kahn, R., and Koutrakis, P.: Using aerosol optical thickness to predict ground-level $PM_{2.5}$ concentrations in the St. Louis area: A comparison between MISR and MODIS, Remote Sens. Environ., 107, 33–44, 2007.

Lui, Y., Koutrakis, P., and Kahn, R.: Estimating fine articulate matter component concentrations and size distributions using satellite-retrieved fractional aerosol optical depth: Part 1 – Method Development, Air Waste Manage. Assoc., 57, 1351–1359, 2009a.

Lui, Y., Koutrakis, P., Kahn, R., Turquety, R., and Yantosca, R. M.: Estimating fine particulate matter component concentrations and size distributions using satellite-retrieved fractional

ACPD
11, 30563–30598, 2011

aerosol optical depth: Part 2, J. Air Waste Manage. Assoc., 57, 1360–1369, 2009b.
McMurry, P., Shepherd, M., and Vickery, J.: Particulate Matter Assessment for Policy Makers: A NARSTO Assessment, Cambridge University Press, Cambridge, England, 2004.
Pelletier, B., Santer, R., and Vidot, J. Retrieving of particulate matter from optical measurements: A semiparametric approach, J. Geophys. Res., 112, D06208, doi:10.1029/2005JD006737, 2007.
Pope, C. A., Ezzati, M., and Dockery, D. W.: Fine-particulate air pollution and life expectany inthe United States, N. England J. Med., 360, 376–386, 2009.
Remer, L. A., Kaufman, Y. J.,Tanré, D., Mattoo, S., Chu, D. A., Martins, J. V., Ichoku, C., Levy, R. C., Kleidman, R., Eck, T. F., Vermote, E., and Holben, B. N.: The MODIS Aerosol Algorithm, Products and Validation, J. Atmos. Sci., 62, 947–973, 2005.
Samet, J. M., Dominici, F., Curriero, F. C., Coursac, I., and Zeger, S. L.: Fine particulate air pollustio and mortality in 20 U.S. cities, 1987–1994, N. Engl. J. Med., 343, 1742–1749, 2000.
van Donkelaar, A., Martin, R., Brauer, M., Kahn, R., Levy, R., Verduzco, C., and Villeneuve, P. J.: Global estimates of ambient fine particulate matter concentrations form satellite-based optical depth: Development and application, Environ. Health Persp., 118, 847–855, 2010.
Vidot, J., Santer, R., and Ramon, D.: Atmsopheric particulate matter (PM) estimation from SeaWiFS imagery, Remote Sens. Environ., 111, 1–10, 2007.
Wang, J. and Christopher, S. A.: Intercomparison between satellite-derived aerosol optical thickness and $PM_{2.5}$ mass: Implications for air quality studies, Geophys. Res. Lett. 30, 2095, doi:10.1029/2003GL018174, 2003.
Watson, J. G., Chow, J. C., Bowen, J. L., Lowenthal, D. H., Hering, S., Ouchida, P., and Oslund, W.: Air quality measurements from the Fresno Super Site, J. Air Waste Manage. Ass., 50, 1321–1334, 2000.
Wood, S. N.: Generalized Additive Model: An introduction with R, Chapman & Hall/CRC, Boca Raton, 2006.
Wood, S. N.: Fast stable direct fitting and smoothness selection for Generalized Additive Models, arXiv:0709.3906v1, Cambridge University Press, 2007.
Zhu, K., Zhang, J. F., and Lioy, P. J.: Evaluation and comparison of continuous fine particualte matter nomitors for measurement of ambient aerosol, J. Air Waste Manage. Assoc., 57, 1499–1506, 2007.

ACPD
11, 30563–30598, 2011

Table 1. List of sites used in this study and their latitude and longitude.

Site	Latitude	Longitude
Bakersfield	35.36° N	−119.06° W
Fresno	36.78° N	−119.77° W
Modesto	36.64° N	−120.99° W
Stockton	36.95° N	−121.27° W
Tracy	36.68° N	−121.44° W
Turlock	36.48° N	−120.84° W

ACPD
11, 30563–30598, 2011

Table 2. Correlation coefficients (R^2) for linear regressions between response and parameter. Data from all sites.

Response	Parameter	R^2
AOD_47	AOD_55	0.97
AOD_47	DB_AOD_47	0.35
AOD_47	OMI_AOD	0.15
AOD_47	Ang_Exp	0.7e-6
DB_AOD_47	DB_AOd_55	0.97
DB_AOD_47	OMI_AOD	0.07
OMI_AOD	OMI_AAOD	0.6
OMI_AOD	OMI_VAI	0.17
PM_{25}_Hourly	AOD_47	0.14
PM_{25}_Hourly	DB_AOD_47	0.16
PM_{25}_Daily	AOD_47	0.01
PM_{25}_Daily	DB_AOD_47	0.04
PM_{25}_Hourly	OMI_AOD	0.004
PM_{25}_Hourly	OMI_NO_2	0.05

ACPD
11, 30563–30598, 2011

Table 3. Correlation coefficients for individual sites using a linear fit between MODIS AOD and $PM_{2.5}$ and the gam model. (See text for details.)

	Bakersfield[2]	Fresno	Modesto[1]	Stockton[1]	Tracy[3]	Turlock[1]
R^2 for gam	0.44	0.72	0.55	0.50	0.56	0.48
No. of Points	555	359	551	392	76	196
R^2 of linear fit	**0.07**	**0.21**	**0.28**	**0.24**	**0.07**	**0.22**

[1] no AAOD or DB because they reduced the no of points too much.

[1] no AAOD or AOD because they reduced the no of points too much.

[3] PM_{25} only existed for part of 2007 in Tracy.

Signif. codes: 0 '***' 0.001 '**' 0.01 '*' 0.05 '.' 0.1 ' ' 1

ACPD
11, 30563–30598, 2011

Table 4. Correlation coefficients derived for various gam models and parameter *p*-values. Data from all sites. (see text for gam model details.)

	GAM1	GAM2	GAM 3	GAM 4	GAM 5	GAM 6	Combined
AOD	83-13	NA	<2e-16	2.5e-16	NA	<2e-16	
DB	2e-13	<2e-16	NA	<2e-16	<2e-16	NA	
OMI_AOD	.05	.013	.04	3.3e-3	4.5e-6	2e-11	
AAOD	2e-4	1.0	4.3e-10	NA	NA	NA	
NO2	.12	3.3e-09	1.2e-4	4.2e-4	1e-14	2.6e-12	
doy	<2e-16	<2e-16	<2e-16	<2e-16	<2e-16	<2e-16	
r^2 for gam	0.74	0.66	0.71	0.67	0.63	0.63	0.69
No. of Points	630	1037	1345	943	1483	2122	1272
r^2 for linear fit	**0.08**	**0.16**	**0.18**	**0.1**	**0.17**	**0.17**	**0.09**

[1] no AAOD or DB because they reduced the no of points too much.

[2] no AAOD or AOD because they reduced the no of points too much.

[3] PM_{25} only existed for part of 2007 in Tracy.

Signif. codes: 0 “***” 0.001 “**” 0.01 “*” 0.05 “.” 0.1 “ ” 1

ACPD
11, 30563–30598, 2011

Table 5. Effect of adding observation type on the number of data points with valid data.

	Observation type	No. of Days
A	Days in series	8244
B	Total MODIS days	4455
C	Total valid 5 × 5 MODIS days	4340
D	Days in row C w/o PM_{25}_Hourly	1299
E	Days in row C w/o PM_{25}_Daily	1697
F	Days in row C w/o MODIS _AOD	97
G	Days in row C w/o MODIS_DB_AOD	1993
H	Days in row C w/o OMI_NO2	230
I	Days in row C w/o OMI_AOD	531
J	Days in row C w/o OMI_AAOD	1955

ACPD
11, 30563–30598, 2011

Fig. 1. Map of the San Joaquin Air Pollution Control District in California highlighting the coverage provided by ground sites and satellites.

ACPD
11, 30563–30598, 2011

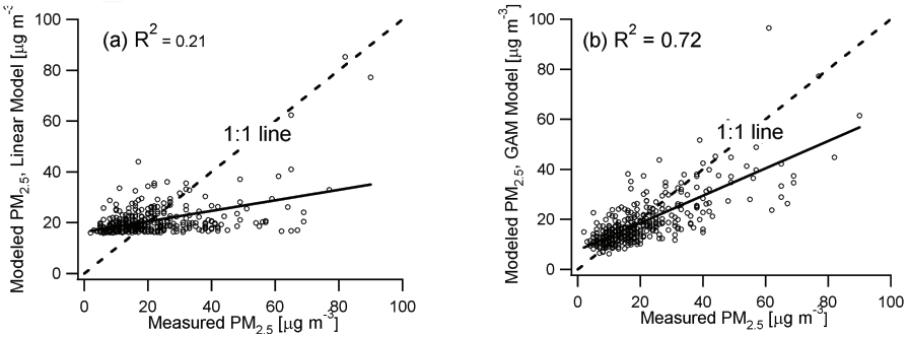

Fig. 2. Comparison of modeled vs measured $PM_{2.5}$ using a linear **(a)** and GAM model **(b)**.

ACPD
11, 30563–30598, 2011

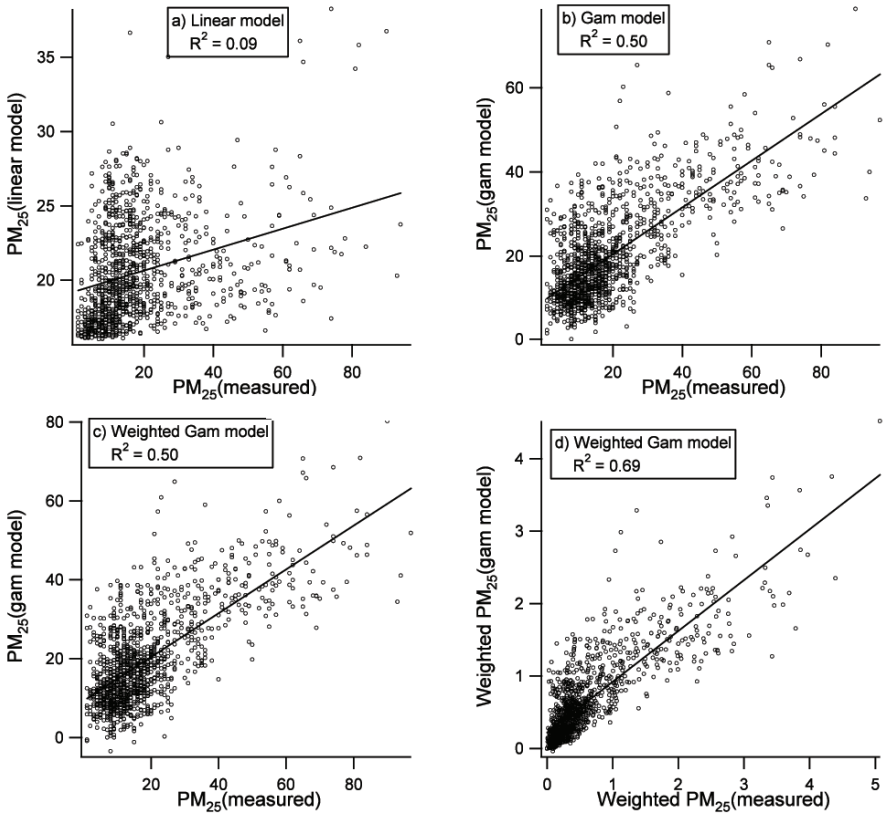

Fig. 3. Comparison of modeled/measured PM_{25} correlations for three different models. **(a)** the simply linear regression model. **(b)** The composite gam model. **(c)** The weighted gam model. **(d)** The weighted gam model plotted in weighted space.

ACPD
11, 30563–30598, 2011

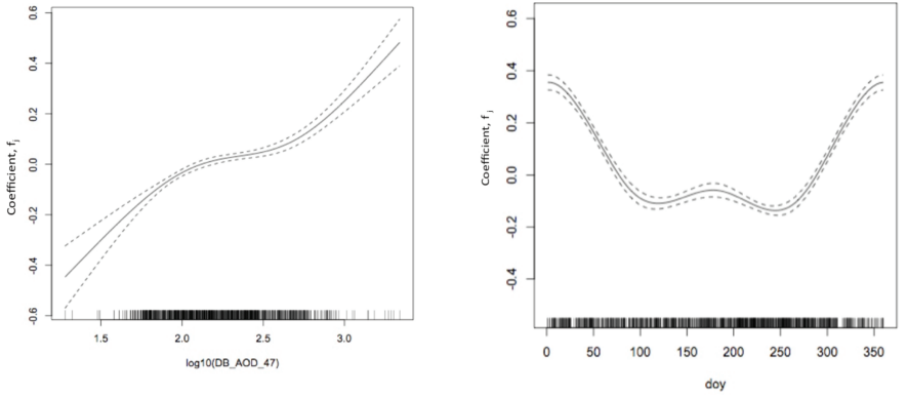

Fig. 4. Plot showing nearly linear relationship between $PM_{2.5}$ and two of the GAM parameters. These coefficients correspond to the f_j in Eq. (4). **(a)** MODIS Deep Blue AOD; **(b)** seasonality parameter, "doy".

ACPD
11, 30563–30598, 2011

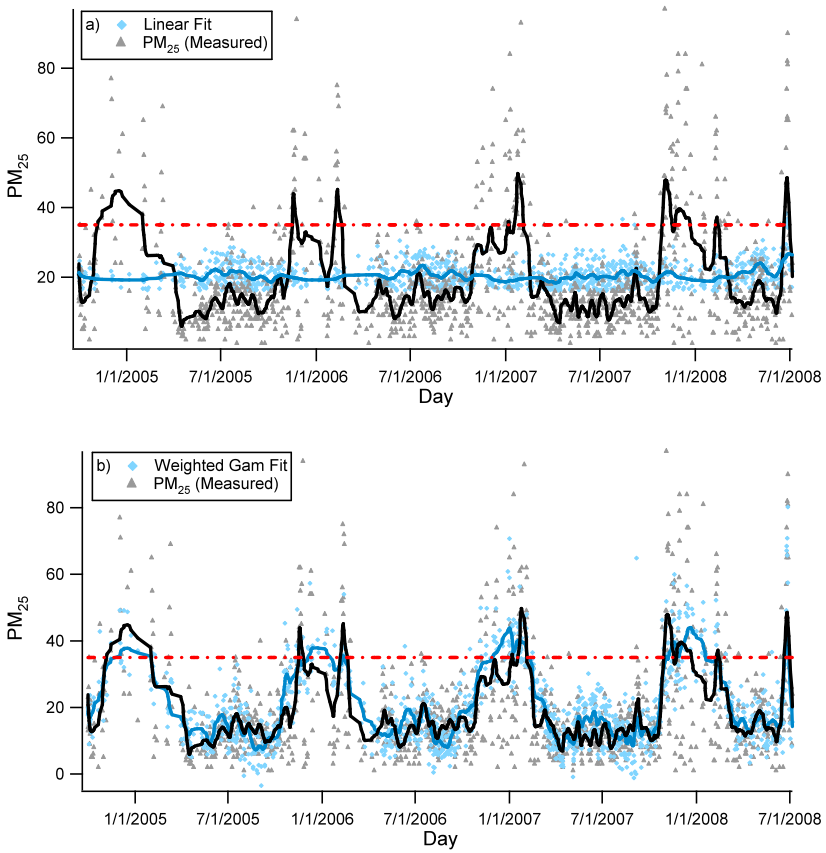

Fig. 5. Trends of retrieved and measured PM in SJV. The EPA 24-h criterion is shown as a red dashed line. The blue and gray points are the retrieved and measured $PM_{2.5}$, respectively. The blue and black solid lines are loess fits to the retrieved and measured and $PM_{2.5}$, respectively.

ACPD
11, 30563–30598, 2011